Supplementary Information

1. Crystal structure of boron carbide

Boron carbide, a α-rhombohderal boron-rich compound with space group of $R\bar{3}m$ (No.166), is a non-stoichiometric compound, its rhomohedral lattice parameters, a_r and α_r , change with the carbon atomic percentage [1, 2]. The rhombohedral unit cell of boron carbide consists of eight icosahedral clusters (B_{12} or $B_{11}C$, etc.) at the corners and a 3-atom chain (possibly C-B-C or C-B-B, etc.) along the diagonal[1, 3-6]. The crystal structure of boron carbide can be considered as a distorted cubic close packing (CCP) of icosahedral clusters. Its rhombohedral unit cell can be compared to a rhombohedral primitive unit cell of a face centered cubic (FCC) variant of the CCP structure [Fig. S1]. For boron carbide, its close packing plane of icosahedral clusters is $\{100\}_r$ and it is equivalent to the $\{100\}_{fcc}$-type crystal plane of CCP.

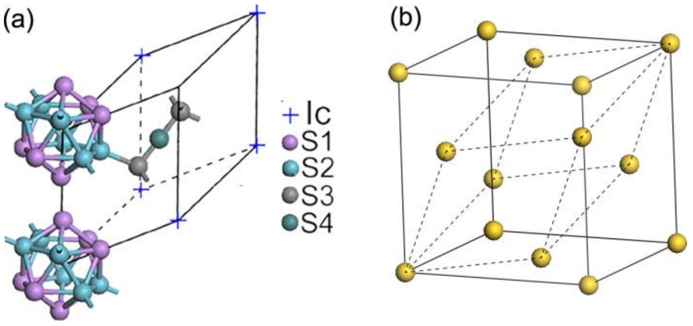

Fig. S1 (Color online) (a) Boron carbide rhombohedral unit cell. S1-S4 represents four atomic sites in the unit cell, respectively, and the cross line is the simplified symbol for icosahedral atomic cluster (Ic). (b) FCC unit cell defined by solid lines and its primitive cell consisting of six $\{100\}_{fcc}$-type close-packing planes outlined by the dashed lines.

2. Experimental geometry and diffraction pattern registration for the reconstruction of the reciprocal 3D volume

The experimental geometry and procedures of 3D electron diffraction mapping for five-fold twinned nanostructures are illustrated in Fig.S2. The axis of the nanowire, i.e. the $[001]_r$ direction, is defined as the rotation axis (RA). The nanowire is firstly rotated around its RA to a mirror-symmetric orientation with respect to the incident electron beam, then the direction orthogonal both to the axis of the nanowire (i.e. RA) and the incident electron beam is set as the tilting axis (TA) [Fig. S2(a)]. To facilitate the subsequent experimental operation and data analysis, TA should been aligned with a tilting axis of the specimen holder before beginning the systematic tilting and data acquisition. For the common used double-tilt holder without *in-situ* rotation capability, TA can be aligned with one of the tilting axes of the holder through *ex-situ* specimen-rotating by using a marked grid to locate the position of the nanowire. Subsequently a series of mirror-symmetric diffraction patterns could be recorded by tilting the nanowires along TA with a regular tilt step of 0.1° [Fig. S2(b)].

The diffraction patterns collected show a common feature in the equatorial line consisting of a systematic row of diffraction spots diffracted by a set of $(1\bar{1}0)_r$ planes of T1 and a set of $(100)_r$ planes ($(0\bar{1}0)_r$ planes) of T3 (T4) [Fig. S2(c)]. These tilt-invariant diffraction spots provide the reference for pattern registration for the reconstruction of the 3D diffraction intensity map for the five-fold cyclic twinned nanowire [Fig. S2(d)]. Fig. 1(c) shows a reconstructured reciprocal volume containing the $(112)_r$ and $(113)_r$ reflections of a boron carbide five-fold cyclic twinned nanowire. From the reconstructured reciprocal volume, an extracted slice labelled as Ω traversing five $(112)_r$ Bragg reflection centers has be used to retrieve the information about the cross-sectional morphology and internal structure about the five-fold twinned nanowire. Given the original point of tilting angle ($\theta_{\mathrm{TA}}=0°$) at the orientation that the axis of the nanowire ($[001]_r$ direction) is perpendicular to the incident electron beam, experimentally the angular range of systematic tilting should be set from about $\theta_{\mathrm{TA}}=-10°$ to $\theta_{\mathrm{TA}}=10°$ to make sure that the reciprocal-space volume spanned by the pivoting surface of the Ewald sphere will cover the $(112)_r$ diffraction intensity distributions of all five crystalline segments.

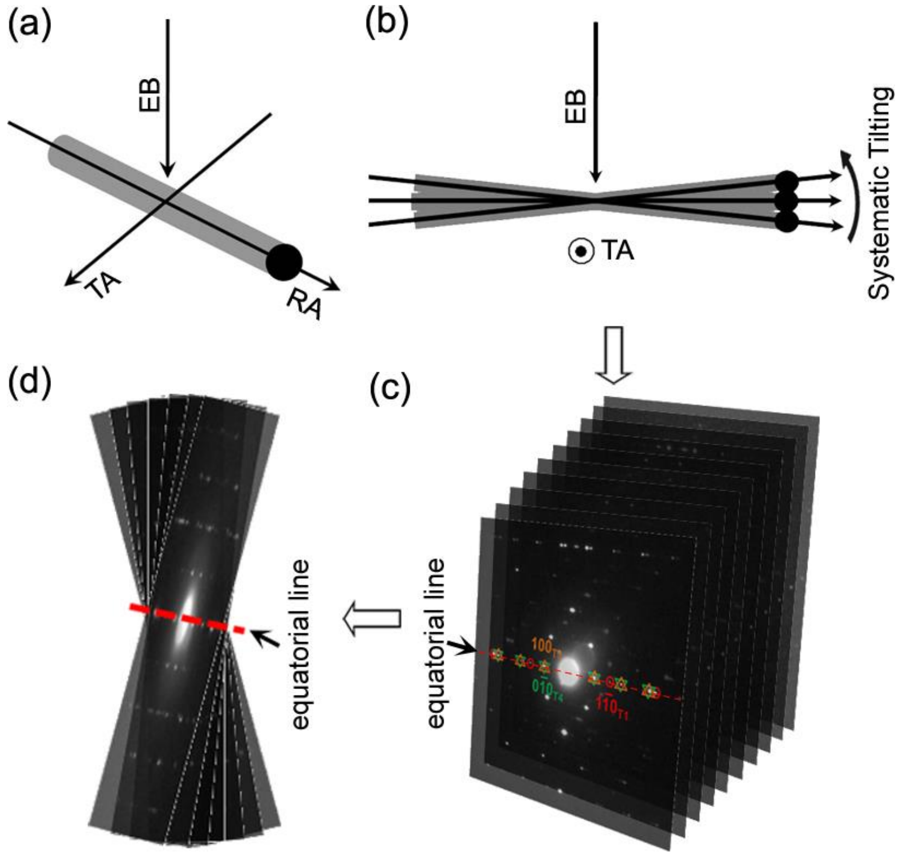

Fig.S2 (Color online) Experimental setup of 3D electron diffraction mapping for five-fold cyclic twinned nanowires: (a) Orientation relationship of the rotation axis (RA), the tilting axis (TA) and the incident electron beam; (b) Orientation of the systematic tilting axis applied; (c) The diffraction stack taken as a function of the tilting angles; (d) The relative relationship of the diffraction patterns, corresponding to the intersection of the Ewarld sphere with the diffraction peaks in the reciprocal space.

Experimentally, 3D electron diffraction mapping for boron carbide five-fold cyclic twinned nanowires was carried out using a JEM-2010 transmission electron microscope with a LaB_6 filament operated at the 200KV electron accelerating voltage. A series of electron diffraction patterns was collected in the selected area electron diffraction mode with a selected area aperture of a diameter about 150nm. To make sure that all the electron diffraction patterns were recorded from the same region of the boron carbide nanowire, a region with easily identifiable feature (for example, the tail area of a nanowire without the supporting carbon film) was selected before the acquisition of electron diffraction data, rechecked after the selected area diffraction has be recorded. Selected electron diffraction patterns were collected by a 14-bit Gatan 831 charge-coupled device (CCD) camera, all at the same acquisition condition and the same parallel beam illumination setting.

3. Data process for 3D reciprocal volume visualization

To visualize 3D reciprocal volume containing the $(112)_r$ reflections under consideration, we needed to transform the irregularly shaped volume element sampled by the Ewarld sphere during the systematic tilting experiment into regular rectilinear volume elements (voxels). This is achieved using a 3D matrix transformation method using a Matlab script. The scheme can be simply summarized into 3 steps. Firstly, we extracted the 2D intensity information about the $(112)_r$ reflections from the recorded diffraction patterns. Every slice of 2D map of $(112)_r$ reflections corresponds to a rectangular area with same pixel size and offset the same distance from the equatorial line. As shown in Fig. S3 (a) viewing along the direction of the equatorial line, the extracted data set corresponds to a volume with sectorial cross section in reciprocal space. This set of extracted 2D maps can be incorporated into a 3D matrix [Fig. S3 (b)]. The direct visualization of the 3D matrix is a cuboid volume which is the distortion of the real reciprocal-space volume [Fig. S3(a)] for data acquisition. Therefore, further mathematic process is necessary to correct this distortion. Secondly, the 2D reciprocal slice has been shifted along the Y axis to correct the curvature as shown in Fig. S3 (c). Lastly, interpolation along the X direction has been carried out to maintain the same size per pixel along the X direction for multiple 2D slice in the X-Z plane [Fig. S3(d)].

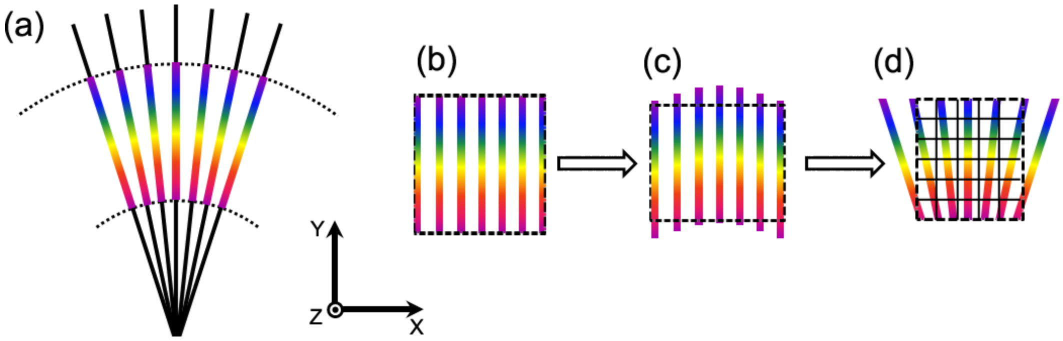

Fig. S3 (Color online) (a)Schematic view of a tilt series of diffraction patterns aligned along equatorial line (parallel to the Z axis in this figure). The black line with a rainbow colored section represents a slice of diffraction pattern. The rainbow colored section symbolically indicated the area of interest in the raw data. (b)-(c) demonstrated the mathematical process applied to raw data set within the area of interest. (b) The 3D matrix representation slice-by-slice of the extracted 2D mapping from a tilt series of diffraction patterns. (c) The vertical shift of the 2D slices in the Y-Z plane along the Y direction. (d) The interpolation of the shifted 2D slices in the X-Z plane along the X direction.

4. Rhombohedral lattice parameters refinement of the boron carbide five-fold cyclic twinned nanowire under investigation in this paper

The lattice parameters of an individual boron carbide nanowire shown in the inset of Fig. 2 (c) with diameter about 80nm have been determined by indexing the zone-axis diffraction patterns. As shown in Fig.S4, two such diffraction patterns have been indexed to be $[100]_{T3}$ & $[010]_{T4}$ and $[1\text{-}10]_{T2}$, respectively. According to the analysis obtained from the experimental diffraction patterns [Fig.S4 (b) and (d)], rhombohedral lattice parameters of the nanowire have been refined as

a_r =5.17Å, α_r=67°. As demonstrated in Table S1, the calculated interplanar spacing and dihedral angle between different crystallographic planes in terms of the refined lattice parameters are matched with the measured results from the experimental electron diffraction patters [Fig. S4 (b) and (d)].

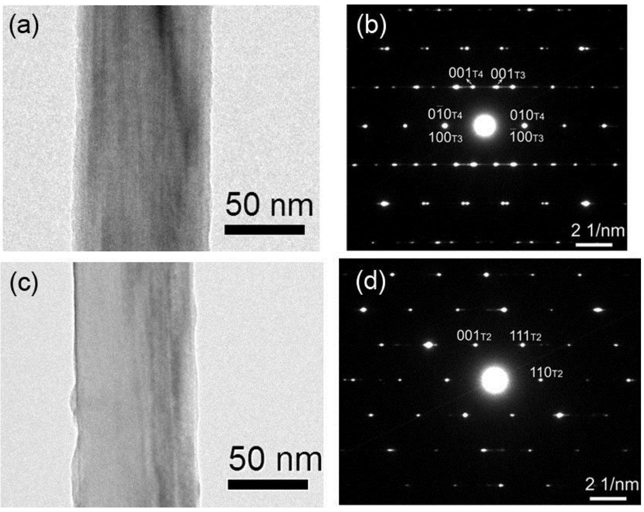

Fig. S4. Experimental diffraction patterns and the corresponding bright field (BF) morphology images from the five-fold twinned nanowire for electron diffraction tomography in this paper. The five crystalline segments are consecutively labeled as T1~T5. (a)-(b) BF image and the corresponding diffraction patter viewing down the $[100]_{T3}$ and $[010]_{T4}$ zone-axis, respectively. (c)-(d) BF image and corresponding diffraction pattern viewing down the $[1\text{-}10]_{T2}$ zone-axis, respectively.

Table S1. Comparison between experimental crystallographic results (Exp.) determined by indexing diffraction patterns [Fig. S2] and the corresponding theoretical results (Theo.) calculated by the refined rhombohedral lattice parameters.

	d-spacing(Å)			Angle between 2 planes (°)		
	$d_{(001)}$	$d_{(110)}$	$d_{(111)}$	$(100)/(0\bar{1}0)$	(110)/(111)	$(\bar{1}\bar{1}0)/(001)$
Exp.	4.5(6)	3.8(3)	3.9(8)	73.(7)	50.(4)	62.(4)
Theo.	4.57	3.81	3.98	73.7	50.4	62.1

5. Extinction distance evaluation of $(112)_r$ reflection of boron carbide

According to the equation, $\xi_g = (\pi V_c \cos\theta) / (\lambda F_g)$ [7], the evaluated extinction distance for a $(112)_r$ reflection of boron carbide is about 180nm at 200 kV (λ=0.0251Å). The volume of rhombohedral boron carbide unit cell is estimated to be 109.60 Å^3. For the evaluation of the structure factor ($F_{hkl} = \sum_i f_i e^{2\pi i(hx_i + ky_i + lk_i)}$) for boron carbide $(112)_r$ reflection, the electron scattering factors of boron and carbon atom are taken from the tabulated value calculated by relativistic Hartree-Fock method[8].

The large extinction distance means that we can treat the corresponding diffraction from each of the crystallites whose size is less than 50nm in any direction as largely kinematical, to the first approximation.

References

1. H. Werheit, *Boron compounds, Numerical Data and Functional Relationships in Science and Technology*, Springer-Verlag, Berlin, 2000.
2. T. L. Aselage and R. G. Tissot, *Journal of the American Ceramic Society*, 1992, **75**, 2207-2212.
3. D. Emin, *Physical Review B*, 1988, **38**, 6041-6055.
4. Y. Feng, G. T. Seidler, J. O. Cross, A. T. Macrander and J. J. Rehr, *Physical Review B*, 2004, **69**, 125402.
5. F. Mauri, N. Vast and C. J. Pickard, *Physical Review Letters*, 2001, **8708**, 085506.
6. R. Lazzari, N. Vast, J. M. Besson, S. Baroni and A. Dal Corso, *Physical Review Letters*, 1999, **83**, 3230-3233.
7. D. B. Williams and C. B. Carter, *Transmission Electron Microscopy: A Texbook for Materials Science*, Plenum Press, New York, 1996.
8. P. A. Doyle and P. S. Turner, *Acta Crystallographica Section A*, 1968, **24**, 390-397.